

CHEMICAL PHYSICS  
OF BIOLOGICAL PROCESSES

**Comparative Analysis of Physicochemical Characteristics  
of Fluorophore Groups of Lipofuscin Granules  
from Retinal Pigment Epithelium Cells of Human Cadaver Eyes  
in Normal and Pathology**

**M. A. Yakovleva<sup>a, \*</sup>, A. Sh. Radchenko<sup>a</sup>, A. A. Kostyukov<sup>a</sup>, V. V. Chagovets<sup>b</sup>, A. S. Kononikhin<sup>a, c</sup>,  
M. Kh. Khubetsova<sup>d</sup>, S. A. Borzenok<sup>d</sup>, V. A. Kuzmin<sup>a</sup>, E. N. Nikolaev<sup>c</sup>,  
T. B. Feldman<sup>a, e</sup>, and M. A. Ostrovsky<sup>a, e</sup>**

<sup>a</sup> Emanuel Institute of Biochemical Physics, Russian Academy of Sciences, Moscow, Russia

<sup>b</sup> Kulakov National Medical Research Center for Obstetrics, Gynecology, and Perinatology,  
Ministry of Health of the Russian Federation, Moscow, Russia

<sup>c</sup> Skolkovo Institute of Science and Technology, Moscow, Russia

<sup>d</sup> Fyodorov Eye Microsurgery, Ministry of Health of the Russian Federation, Moscow, Russia

<sup>e</sup> Moscow State University, Moscow, Russia

\*e-mail: lina.invers@gmail.com

Received July 27, 2021; revised August 13, 2021; accepted August 20, 2021

**Abstract**—A comparative study of individual groups of bisretinoids and their oxidation and degradation products in chloroform extracts from cells of the retinal pigment epithelium (RPE) of human cadaver eyes without signs of pathology (norm) and in the case of visualized age-related macular degeneration is carried out. Fluorescence analysis and high-performance liquid chromatography-mass spectrometry show that with age-related macular degeneration, an increased content of oxidation and degradation products of bisretinoids are observed in comparison with the norm. The results obtained allow us to conclude that the listed methods can be used in the preclinical diagnosis of degenerative diseases of the retina and the RPE of the human eye.

**Keywords:** lipofuscin granules, fluorophores, retinal pigment epithelium, autofluorescence, method of calculating time-correlated photons

**DOI:** 10.1134/S199079312201033X

## INTRODUCTION

Degenerative diseases of the retina and retinal pigment epithelium (RPE) of the human eye are one of the main causes of complete or partial loss of vision. The most common and socially significant disease is age-related macular degeneration (AMD) [12]. In the mechanisms of aging and degeneration of the retina and the RPE, the most important role belongs to the so-called old age pigment, lipofuscin granules (LGs) [3], formed in the RPE cells as a result of the incomplete lysosomal degradation of photoreceptor debris [4]. It is assumed that the development of AMD may be related to the progressive accumulation of LGs. Elevated LG levels in the RPE cells can be considered one of the risk markers for AMD.

Lipofuscin granules contain more than two dozen fluorophores, which are mainly derivatives of all-trans-retinal (bisretinoids and their oxidation products) [5]. The most studied ones among them is bisretinylideneethanolamine (A2E) [6]. Upon absorption of

visible light, they are able to generate a reactive oxygen species (ROS), which determines their phototoxicity [7]. Also, under the action of light and in the presence of oxygen in LGs, the photooxidation of bisretinoid fluorophores can occur with the formation of cytotoxic aldehydes and ketones [5].

One of the promising methods for diagnosing degenerative diseases of the retina and the RPE, including pathology, is the non-invasive fundus autofluorescence (AF) imaging method. However, it should be noted that the AF method makes it possible to diagnose pathology with manifested clinical signs. Therefore, at present, for preclinical diagnostics, they are trying to improve the AF method to extract additional information from the total autofluorescence. A promising approach for this is to measure the fluorescence lifetimes (FLT) when recording them at certain wavelengths: the Fluorescence Lifetime Imaging Microscopy (FLIM) method [8, 9]. One of the main tasks when introducing the FLIM method to ophthal-

mological practice is to determine the composition and fluorescent characteristics fluorophores of LGs in AMD (hereinafter, pathology) compared to the norm.

We have previously shown [10, 11] that AMD is accompanied by an increased content of products of the photooxidation and photodegradation of bisretinoids in comparison with the norm. In addition, the data obtained from the analysis of FLTs [12–14], which showed that the numerical values of the FLTs in both cases did not differ significantly; however, with a pathology, the contribution of longer lived oxidized bisretinoids increased compared to the norm.

Thus, given that the fluorescence characteristics of oxidized and unoxidized forms of LG fluorophores have significant differences, and their relative content changes noticeably in the case of a pathology compared to the norm [10, 11], further detailed study of this phenomenon can make it possible to use these data for the creation of preclinical diagnostics of AMD and other degenerative diseases of the eye.

In this study, we carried out a comparative analysis of the composition of unoxidized and oxidized bisretinoids in separate fractions of a chloroform extract obtained from the RPE cells of human cadaver eyes without signs of pathology and with visualized AMD. To determine the composition of fluorophores, a tandem of methods of mass spectrometry and HPLC analysis were used [15–17]. To analyze the spectral characteristics, the methods of fluorescence analysis and recording of the kinetics of fluorescence decay were used.

## EXPERIMENTAL

**Reagents.** We used reagents and solvents from Sigma-Aldrich, Fluka, and Component-reagent.

**Material.** Cadaveric human eyes were obtained from the Eye Tissue Bank of Fyodorov Eye Microsurgery, Ministry of Health of the Russian Federation based on an agreement on scientific cooperation between the Institute of Biochemical Physics of the Russian Academy of Sciences and Fyodorov Eye Microsurgery [10]: two eyes from a 74-year-old donor without clinical signs of the RPE pathology (norm) and two eyes from a 75-year-old donor with a visualized AMD pathology (pathology).

**Obtaining chloroform extracts from the RPE cells containing bisretinoids and their derivatives.** The RPE was extracted from cadaver eyes according to the technique described in [10]. Retinoid LG fluorophores were extracted from the RPE cells according to the Folch method with a chloroform-methanol mixture (2 : 1) [18].

**HPLC analysis.** Chromatographic separation of bisretinoids and products of their photooxidation and photodegradation in chloroform extracts of the RPE was carried out on a Knauer chromatograph (Germany) with a Diasfer 110-C18 column (4 × 250 mm,

sorbent size 5 μm) of BioKhimMak ST (Russia), as described earlier in [13]. Bisretinoid A2E synthesized according to the method described in [19] was used as the standard.

As a result of the HPLC analysis of chloroform extracts, fractions containing separate groups of retinoids were obtained. Fraction 1 was obtained at retention times of 2 to 5 min; fraction 2, 7–16 min; and fraction 3, 18–25 min (see Fig. 1 below).

**Measurement of fluorescence spectra.** Fluorescence spectra were recorded on an RF-5301PC spectrofluorimeter (Shimadzu, Japan).

**Registration of fluorescence decay kinetics.** The FLT of the chloroform extract of the RPE was measured by counting time-correlated photons using a FluoTime 300 spectrofluorimeter (PicoQuant, Germany) at the Center for Shared Use “New Materials and Technologies” of the Institute of Biochemical Physics, Russian Academy of Sciences. The fluorescence of the sample was excited using a PicoQuant diode laser (Germany) LDH-PC-485 (485 nm, pulse duration 107 ps). The fluorescence signal was recorded at a wavelength of 556 nm. The kinetic curves of fluorescence decay were processed within the three-exponential model. The FLT and the contribution of individual groups of fluorophores to the detected fluorescence decay curves were calculated using the following formula, taking into account the instrument response function (IRF):

$$I(t) = \int_{-\infty}^t IRF(t') \sum_i A_i \exp((-t - t')/\tau_i) dt',$$

where  $i$  is the component number,  $A$  is the amplitude, and  $\tau$  is the FLT. It should be noted that in this study, we used the amplitude ( $A$ ) parameter, and not intensity, since the purpose of this analysis was to show the relative content of the investigated substances, which is displayed by the amplitude.

For the experiment, the samples were preliminarily evaporated with the use of the chemical vacuum system MZ 2C NT + AK + M + D (Vacuubrand, Germany), and then dissolved in 1 mL of chloroform ( $D_{485} = 0.08–0.2$ ). Data analysis was carried out using the FluoFit software (PicoQuant, Germany).

**HPLC with mass spectrometric detection.** Chloroform extracts from the RPE were analyzed by HPLC with mass spectrometric (HPLC-MS) detection on a Dionex UltiMate 3000 chromatograph (Thermo Fisher Scientific, Germany) and a MaXis impact mass spectrometer (Bruker, Germany). Separation was carried out by the hydrophilic interaction chromatography (HILIC) method on a Waters (United States) SpherisorbSilica column (1 × 250 mm; sorbent size, 5 μm) with the following gradient: 0–0.5 min, 94% A, 6% B; 0.5–60.5 min, 77% A, 23% B; and 61–64 min, 94% A, 6% B, where A is acetonitrile, B is ammonium acetate, 5 mmol/L. The flow rate was 50 μL/min.

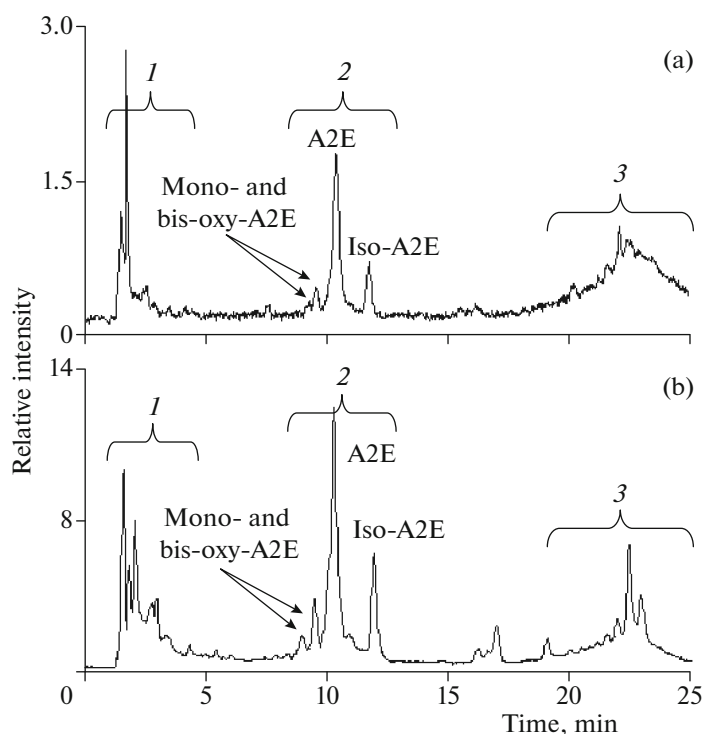


**Fig. 1.** HPLC analysis of chloroform extracts from the RPE of two eyes of a donor aged 74 years without signs of pathology (a) and two eyes of a 75-year-old donor with visualized AMD (b). Peak groups: (1) products of photooxidation and photodegradation of bisretinoids [10]; (2) A2E, iso-A2E, mono-, and bis-oxy-A2E [20]; (3) modification products fully-*trans*-retinal and their slightly oxidized products [5, 21, 22]. Detection by absorption at a wavelength of 430 nm.

Mass spectrometric analysis was performed with electrospray ionization and mass spectra were recorded in the positive ion mode in the range  $m/z$  from 400 to 1000. The parameters of the ion source: the voltage across the needle was 4200 V, the spraying gas was supplied at a pressure of 0.7 bar, and the drying gas flow was 6 L/min at a temperature of 200°C.

## RESULTS AND DISCUSSION

### *Comparative HPLC Analysis of Retinoids from the RPE Cells of Eyes of Donors without Signs of Pathology and with Visualized AMD*

Figure 1 shows the results of the HPLC analysis of chloroform extracts from the RPE of two donor eyes without signs of pathology (a) and two donor eyes with visualized AMD (b). The group of peaks 1 on the chromatograms corresponds to products of the photooxidation and photodegradation of bisretinoids [10]. The group of peaks 2 corresponds to A2E and iso-A2E, as well as the products of their mono- and bis-oxidation [20]. Peak group 3 (according to the published data) can correspond to bisretinoids such as A2-DHP-PE, A2-DHP-E [5], RAL-dimer, RAL-dimer-E, A2-GPE, and products of their weak oxidation [21], as well as high-molecular products of the polymerization of bisretinoids [22]. A comparative analysis shows that in the case of AMD in group 1

there are peaks corresponding to diverse products of the photooxidation and photodegradation of bisretinoids. These results are in good agreement with those obtained earlier [10, 11].

### *Comparative Fluorescence Analysis of Chloroform Extracts from RPE Cells from the Eyes of Donors without signs of Pathology and with Visualized AMD*

Figure 2 shows the fluorescence spectra of the studied samples and individual fractions of these chloroform extracts. The individual fractions were obtained as a result of HPLC analysis and correspond to the numbers of the indicated groups of peaks in Fig. 1.

It can be seen from Fig. 2 that in the case of a chloroform extract from the RPE of donor eyes with signs of a pathology, the fluorescence intensity in the short-wavelength part of the spectrum (500–550 nm) is noticeably higher compared to the norm. In the previously published works [10, 11, 13], we assumed that such an increase in the fluorescence intensity in the short-wavelength part of the spectrum occurs due to the increased content of the products of photooxidation and photodegradation of bisretinoids. In this study, in order to test this assumption, we obtained individual fractions of chloroform extracts and recorded their fluorescence spectra (Fig. 2, fractions 1–3). It can be seen from the data obtained that the main contribution to

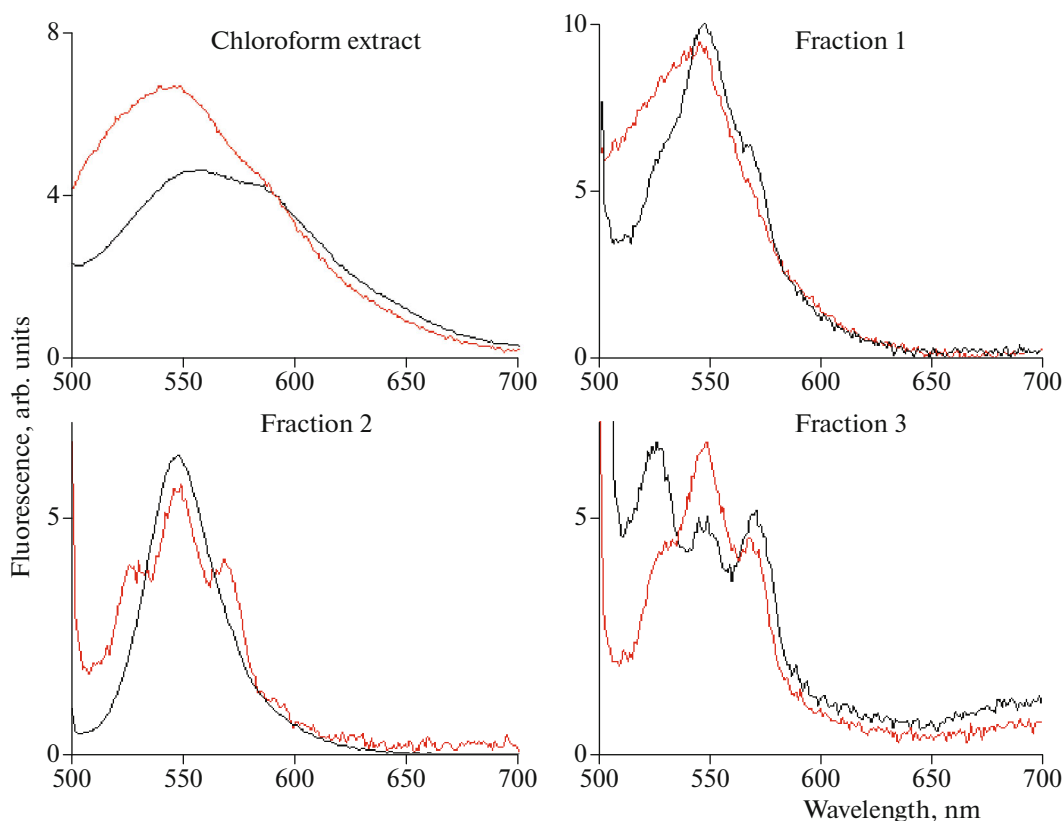


**Fig. 2.** Fluorescence spectra of chloroform extracts from the RPE of donor eyes and individual fractions of these chloroform extracts (fractions 1–3) obtained as a result of HPLC analysis (Fig. 1). Fluorescence was excited with light with a wavelength of 488 nm. Norm, black line of the spectrum; pathology, red line of the spectrum. Fraction (1) products of photooxidation and photodegradation of bisretinoids [10]; fraction (2) A2E, iso-A2E, mono-, and bis-oxy-A2E [20]; fraction (3) modification products fully-*trans*-retinal and their slightly oxidized products [5, 21, 22]. The spectra of chloroform extracts are normalized to a wavelength of 592 nm.

the increase in the fluorescence intensity in the short-wavelength part of the spectrum of the RPE sample from donor eyes with signs of AMD occurs due to the increased content of the photooxidation products and photodegradation of the bisretinoids present in fraction 1 (Fig. 1, group of peaks 1).

*Comparative Analysis of Fluorescence Decay Curves of Individual Fractions of Chloroform Extracts from the RPE Cells of Donor Eyes without Signs of Pathology and with Visualized AMD*

For each fraction obtained from the chloroform extract (Figs. 1, 2), the decay kinetics for the fluorescence was recorded at a wavelength of 556 nm. The FLT and the contribution of individual groups of fluorophores (fractions 1–3) to the detected curves were calculated in the three-exponential model (Table 1).

As shown above, the fluorescence of the chloroform extract from the RPE is mainly due to the LG fluorophores. Currently, more than 20 types of fluorophores have been identified that are all-*trans*-retinal. Therefore, the use of the three-exponential model

gives averaged values when calculating the characteristic FLT. In relation to this, according to the results obtained (Table 1), we can assume that the values of  $\tau_1$ ,  $\tau_2$ , and  $\tau_3$  for different samples are approximately the same and are, on average, 0.18, 3.2, and 6.8, respectively. The obtained times are in good agreement with our previous studies [12, 13], as well as the published data [23].

It can be assumed that the shortest FLT ( $\tau_1$ ) corresponds to unoxidized retinoids from fractions 2 and 3. In fraction 1, they are most likely absent, as indicated by the absence of this temporal component when detecting fluorescence at a wavelength of 556 nm. In other words, fraction 1 contains practically only the products of the photooxidation and photodegradation of retinoids [10].

In this experiment it was impossible to determine the nature of the compounds characterized by time  $\tau_2$ . It would seem that from the data of the chromatographic analysis the main products should be A2E and its isomeric forms. However, according to our studies [10], the contribution of this bisretinoid to the total fluorescence upon excitation by light with a wave-

**Table 1.** Indicators of the FLTs of individual fractions of chloroform extracts from the RPE of donors' eyes without signs of a pathology (norm) and with visualized AMD (pathology); excitation with light at a wavelength of 488 nm, detection at a wavelength of 556 nm

Faction number*		$\tau_1$ , ns	$A_1$ , %	$\tau_2$ , ns	$A_2$ , %	$\tau_3$ , ns	$A_3$ , %
Faction 1	Norm	—	—	3.2	67	7.1	33
	Pathology	—	—	3.4	53	7.6	47
Faction 2	Norm	0.11	33	3.7	62	6.9	5
	Pathology	0.1	20	3.0	55	6.0	25
Faction 3	Norm	0.3	45	2.7	45	6.4	10
	Pathology	0.2	35	2.9	49	6.8	16

\* The numbers of the fractions correspond to the numbers of the groups of peaks in the chromatograms shown in Fig. 1.

length of 488 nm is minimal. At the same time, according to the data of fluorescence analysis, the contribution of the second component ( $\tau_2$ ) is significant. It can be assumed that these compounds can be mono- and/or bis-oxy-A2E (Fig. 1).

The longest-lived component ( $\tau_3$ ), most likely, corresponds to the products of photooxidation and photodegradation of various retinoids (fraction 1). The presence of this component in fractions 2 and 3 can be explained by the contribution of the oxidized A2E forms, as well as weakly oxidized products of the modification of all-*trans*-retinal [21, 22, 14].

Earlier [11, 14], we proposed to determine the presence of a pathology (AMD) by the FLIM method [8, 9] not by the absolute values of the characteristic lifetimes of fluorescence but according to the contribution of individual components, namely, the long-lived component  $\tau_3$ , to the fluorescence decay kinetics.

The results of this study confirmed our assumption that in a pathology the content of the products of the photooxidation and photodegradation of retinoids is higher than in the norm. Analysis of the fluorescence decay curves showed that the contribution ( $A_3$ ) of the longest-lived component ( $\tau_3$ ), which corresponds to these products (fraction 1), increases by 14% in comparison with the norm. It should be noted that a similar trend is observed for fractions 2 and 3. Thus, it has been shown that the products of photooxidation and photodegradation of bisretinoids have the longest FLTs.

*A Comparative Mass Spectrometric Analysis of Individual Fractions of the Chloroform Extract from the RPE cells of Donors' Eyes without Signs of a Pathology and with Visualized AMD*

Figure 3 shows the mass spectra of positive ions, summed over all retention times, for each individual fraction (Figs. 1, 2). As seen from Fig. 3, the most noticeable difference between the mass spectra of the normal and pathology samples is observed in the case of fraction 1. In the case of a pathology, a larger set of intense peaks (10–100% of the maximum intensity

value) is characteristic in comparison with the norm. It should be noted that the results of mass spectral analysis are in good agreement with the chromatographic data and fluorescence detection (Figs. 1, 2). All three types of analysis clearly indicate an increase in the quantitative content and change in the qualitative content of the products of oxidation and degradation of bisretinoids in the case of a pathology.

The values  $m/z$  of the most intense peaks in the mass spectral analysis of the fractions of the chloroform extracts are presented in Table 2. For fraction 1, most of the masses are in the range  $m/z = 400$ – $500$ . According to the published data, the detected substances can be classified as products of the oxidative degradation of bisretinoids [23]. In the mass spectra of fraction 2, the main bisretinoid A2E ( $m/z = 592$ ) and the products of its oxidation ( $592 + n \times 16$ ) with  $m/z = 608, 624, 640, \text{ and } 656$  are detected [10, 20]. The profiles of mass spectra of fraction 3 for the norm and pathology are similar (Fig. 3, fraction 3), which is in good agreement with the data of chromatography and fluorescence detection (Figs. 1, 2). Fraction 3 is characterized by large masses ( $m/z > 700$ ), which can correspond to polymer forms all-*trans*-retinal, as well as bisretinoid dimers and trimmers [22].

Thus, the mass spectrometric analysis showed that the main difference between the norm and pathology in the qualitative and quantitative content of bisretinoids and their oxidation products is observed in fraction 1. In the case of a pathology, the content of products with values  $m/z < 600$  is noticeably greater compared to the norm. Taking into account the results obtained earlier [10], it can be assumed that this fraction mainly contains the products of the oxidative degradation of A2E and other bisretinoids, and that it is the most promising for use as a diagnostic sign of a degenerative disease of the retina.

## CONCLUSIONS

We have previously shown that, in the presence of signs of AMD, the fluorescence spectra of both the RPE suspension and the chloroform extracts of LGs

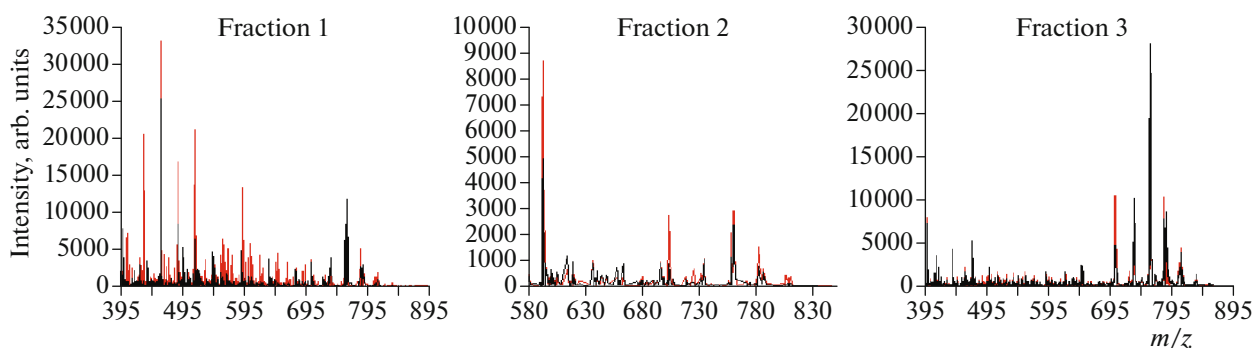


**Fig. 3.** Total mass spectra of positive ions obtained as a result of analysis of chloroform extracts of fractions 1–3. Black lines of mass spectra, norm; red lines of mass spectra, pathology.

from the RPE cells are characterized by more intense fluorescence in the short-wavelength part of the spectrum compared to the norm [10, 11]. In this case, the HPLC analysis showed that in the case of a pathology there is a greater variety and increased relative content of the products of oxidation and degradation of bisretinoids [10, 11]. In addition, in a comparative analysis of the FLT<sub>s</sub> of chloroform extracts, it was found that the values of the characteristic times for the norm and pathology practically do not differ, but the contributions of long-lived components ( $\tau_3$ ) increase in the

case of a pathology [11, 13]. Based on the data obtained, it was assumed that in AMD, the relative content of the oxidation and degradation products of bisretinoids in LGs from the RPE cells is higher than in the norm.

In this study, a comparative study of individual groups of bisretinoids and their oxidation and degradation products for the norm and a pathology was carried out. Fluorescence analysis, HPLC, FLT measurement methods, and mass spectrometry confirmed

**Table 2.** The  $m/z$  values of the most intense peaks\* in the mass spectral analysis of fractions of chloroform extracts of RPE in cadaver eyes without signs of pathology (norm) and with visualized AMD (pathology)

Fraction 1**		Fraction 2**		Fraction 3**	
norm,	pathology	norm	pathology	norm	pathology
400.3	400.3	592.5	592.4	—	413.2
426.4	426.4	608.4	608.3	471.1	471.1
—	428.4	624.5	624.5	—	473.1
459.5	459.5	640.6	640.6	703.6	703.6
—	460.5	656.2	656.2	706.5	704.5
487.5	487.5	703.5	703.6	732.6	—
496.3	—	760.5	760.5	734.6	734.5
—	512.4	783.5	783.5	758.6	758.6
515.5	515.5	—	—	760.5	760.6
—	561.4	—	—	762.6	762.6
—	576.4	—	—	782.6	782.6
—	605.4	—	—	—	784.5
—	693.5	—	—	786.6	786.6
704.6	703.6	—	—	788.6	788.6
758.6	—	—	—	—	806.5
760.6	760.6	—	—	—	810.6
—	782.6	—	—	—	—
786.6	786.6	—	—	—	—

\* The values of the masses of peaks with a relative intensity of 10 to 100% of the maximum intensity value are shown (Fig. 3).

\*\* The numbers of the fractions correspond to the numbers of the groups of peaks in the HPLC analysis of chloroform extracts (Fig. 1).

the earlier assumptions that AMD is accompanied by an increased content of the oxidation and degradation products of bisretinoids in comparison with the norm. The results obtained allow us to conclude that this phenomenon determines the difference in the fluorescent properties of LGs in the normal and pathological conditions, and that it may underlie the development of the spectral analysis of the AF pattern for preclinical diagnosis of degenerative diseases of the retina and RPE of the human eye.

#### FUNDING

This study was financially supported by a grant from the Ministry of Science and Higher Education of the Russian Federation (agreement no. 075-15-2020-773). The equipment and resources of the Center for Collective Use of the Institute of Biochemical Physics, Russian Academy of Sciences “New Materials and Technologies” were used in this study.

#### REFERENCES

- J. R. Sparrow and M. E. Boulton, *Exp. Eye Res.* **80**, 595 (2005).
- F. G. Holz, M. Gross-Jendroska, F. Eckstein, et al., *Ger. J. Ophthalmol.* **4**, 336 (1995).
- C. Kennedy, P. Rakoczy, and I. Constable, *Eye* **9**, 763 (1995).
- F. G. Holz, F. Schutt, J. Kopotz, et al., *Invest. Ophthalmol. Vis. Sci.* **40**, 737 (1999).
- J. R. Sparrow, E. Gregory-Roberts, K. Yamamoto, et al., *Prog. Retin. Eye Res.* **31**, 121 (2012).
- G. E. Eldred and M. R. Lasky, *Nature (London, U.K.)* **361**, 724 (1993).
- M. Boulton, A. Dontsov, J. Jarvis-Evans, et al., *J. Photochem. Photobiol. B* **19**, 201 (1993).
- D. Schweitzer, S. Schenke, M. Hammer, et al., *Microsc. Res. Tech.* **70**, 410 (2007).
- D. Schweitzer, E. R. Gaillard, J. Dillon, et al., *Invest. Ophthalmol. Vis. Sci.* **53**, 3376 (2012).
- T. B. Feldman, M. A. Yakovleva, P. M. Arbukhanova, et al., *Anal. Bioanal. Chem.* **407**, 1075 (2015).
- T. B. Feldman, M. A. Yakovleva, A. V. Larichev, et al., *Eye* **32**, 1440 (2018).
- M. A. Yakovleva, T. B. Fel'dman, P. M. Arbukhanova, S. A. Borzenok, V. A. Kuzmin, and M. A. Ostrovsky, *Dokl. Biochem. Biophys.* **472**, 19 (2017).
- M. A. Yakovleva, A. Sh. Radchenko, T. B. Feldman, et al., *Photochem. Photobiol. Sci.* **19**, 920 (2020).
- M. A. Yakovleva, A. Sh. Radchenko, A. A. Kostyukov, P. M. Arbukhanova, S. A. Borzenok, V. A. Kuzmin, T. B. Feldman, and M. A. Ostrovsky, *Russ. J. Phys. Chem. B* **14**, 462 (2020).
- A. D. Vasilyeva, L. V. Yurina, V. B. Leonova, D. Yu. Azarova, A. E. Bugrova, T. S. Konstantinova, M. I. Indeykina, A. S. Kononikhin, E. N. Nikolaev, and M. A. Rosenfeld, *Russ. J. Phys. Chem. B* **14**, 468 (2020).
- A. S. Kononikhin, N. V. Zakharova, A. E. Yusupov, A. M. Ryabokon, K. Yu. Fedorchenko, M. I. Indeykina, A. E. Bugrova, A. I. Spassky, I. A. Popov, S. D. Varfolomeev, and E. N. Nikolaev, *Russ. J. Phys. Chem. B* **13**, 951 (2019).
- D. G. Ivanov, S. I. Pekov, K. V. Bocharov, D. S. Bor-motov, A. I. Spasskiy, E. S. Zhvansky, A. A. Sorokin, V. A. Eliferov, D. S. Zavorotnyuk, S. I. Tkachenko, I. G. Khaliullin, A. Yu. Kuksin, V. A. Shurkhay, A. S. Kononikhin, E. N. Nikolaev, and I. A. Popov, *Russ. J. Phys. Chem. B* **14**, 483 (2020).
- J. Folch, M. Lees, and G. H. S. Stanley, *J. Biol. Chem.* **226**, 497 (1957).
- C. A. Parish, M. Hashimoto, K. Nakanishi, et al., *Proc. Natl. Acad. Sci. U. S. A.* **95**, 14609 (1998).
- M. A. Yakovleva, N. L. Sakina, A. S. Kononikhin, T. B. Feldman, E. N. Nikolaev, A. E. Dontsov, and M. A. Ostrovsky, *Dokl. Biochem. Biophys.* **409**, 223 (2006).
- S. R. Kim, Y. P. Jang, and J. R. Sparrow, *Vision Res.* **50**, 729 (2010).
- L. S. Murdaugh, L. B. Avalle, S. Mandal, et al., *J. Mass Spectrom.* **45**, 1139 (2010).
- Y. Wu, E. Yanase, X. Feng, et al., *Proc. Natl. Acad. Sci. U. S. A.* **107**, 7275 (2010).